Design of a miniature picosecond low-energy electron gun for time-resolved scattering experiments

R. Karrer, H. J. Neff, M. Hengsberger,[a] T. Greber, and J. Osterwalder
Physik-Institut, Universität Zürich, CH-8057 Zürich, Switzerland

(Received 30 May 2001; accepted for publication 11 September 2001)

We present the design and performance tests of a miniaturized pulsed low-energy electron gun. Electrons photoemitted from a gold cathode are accelerated over a distance of 75 μm and then collimated by a microchannel plate. According to calculations, this novel concept will allow the time spread of the electron pulses to be kept below 5 ps for kinetic energies as low as 100 eV. The achievement of a minimum angular beam divergence ($\approx 1°$) along with an energy resolution of 1.1 eV has to be paid for by low signal intensities. We demonstrate the performance of the gun and the high electron-beam coherence by presenting low-energy-electron diffraction images taken from a submonolayer of lead adsorbed on the germanium (111) surface. We anticipate that this electron gun will open up new possibilities for following structural changes on solid surfaces in real time. [DOI: 10.1063/1.1419219]

I. INTRODUCTION

To follow structural changes during physical and chemical processes in real time is a formidable task. Pump and probe techniques, which became prominent in optical methods (see, e.g., Ref. 1), have been extended in recent years to methods such as x-ray diffraction[2–6] and x-ray absorption fine structure.[7] The probing depth of these methods is of the order of 1000 Å, thus far too much for structural investigations of monolayer-thick films, for instance. The steadily growing interest in structural dynamics in surfaces and interfaces requires the development of a surface-sensitive technique offering high temporal resolution. The penetration depth of electrons in solids can be reduced by choosing large incidence angles or low kinetic energies. Several time-resolved reflection high-energy-electron diffraction studies have been published.[8–11] In these studies, however, the temporal resolution in compromised by the grazing incidence geometry.[9,11]

Low-energy electron diffraction (LEED) is the standard method for structure determination. High scattering cross sections for light elements, large scattering angles, and the analysis of I–V curves and spot profiles to obtain detailed unit cell and morphology information, render LEED a very versatile tool.[12] Adsorbate and substrate dynamics may be disentangled by observing corresponding diffraction spots. Phase transitions and local temperature rise (Debye–Waller factor) manifest themselves as spot intensity transfer into other diffraction spots or diffuse background, respectively.

A time-resolved LEED experiment would consist of a fast change in surface structure induced by a laser pulse (pump) followed by the delayed electron pulse to record the diffraction pattern (probe). The time spread of the electron pulse has, therefore, to match the typical time scale of lattice vibration. An acoustic phonon moving at the velocity of sound (about 1000 m/s), for example, needs some 10 ps to travel over the length scale probed by the LEED ($\approx$100 Å). Vibrational frequencies of molecules adsorbed on solid surfaces, so-called hindered translations, may be of the order of 1 THz,[13] corresponding to a temporal period of 1 ps. Dephasing of coherently excited phonon modes occurs on a scale of some picoseconds.[14] Thus, the time spread Δt of the electron pulses has to be in the low picosecond range. In practice, Δt is determined by

$$\Delta t = \frac{\Delta s}{v} + \frac{\Delta E}{2E}\frac{s}{v}, \tag{1}$$

where v, s, and E are the electron velocity, the path length, and the kinetic energy, respectively, and Δ denotes the respective uncertainties. It can immediately be seen from Eq. (1) that high resolution in time is very difficult to obtain at low electron velocity. The order of magnitude of the different contributions can be estimated as follows: at 100 eV kinetic energy, electrons need 170 ps to travel over a distance of 1 mm. Hence, achieving a 5 ps time spread of the electron pulses means that, according to Eq. (1), for $s=4$ mm and $\Delta E \approx 1.1$ eV, $\Delta s \leqslant 7$ μm.

This condition sets constrains for the design of a pulsed low-energy electron gun. To the best of our knowledge, only ray-tracing calculations have been published so far.[15] In these model simulations, electrons are immediately accelerated to very high energy (typically, some tens of kV), focused by electrostatic lenses and decelerated close to the sample. For practical purposes, however, strong electric-field gradients near the sample are difficult to handle because small deviations from the model geometry destroy the beam characteristics. In our concept, which will be described below, acceleration to high kinetic energy is avoided, and the space between gun and sample is free of electrostatic fields.

[a]Author to whom correspondence should be addressed; electronic mail: matthias@physik.unizh.ch

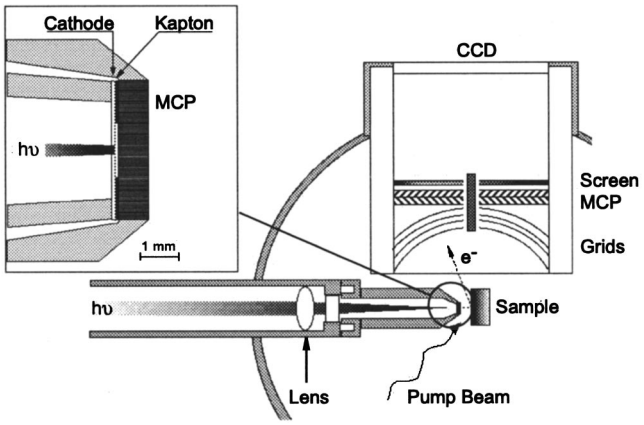

FIG. 1. Setup of the final pump–probe experiment (not to scale). The pump beam arrives from the bottom with 45° incidence onto the surface. The active part of the electron gun is located in the conical end; the laser beam is focused by an external lens and coupled into vacuum through a SiO_2 viewport. Electrons incident normally on the sample surface are backscattered and detected by the LEED optics. Inset: magnified view of the cathode region; the positions of the cathode, collimating MCP, and sample are indicated.

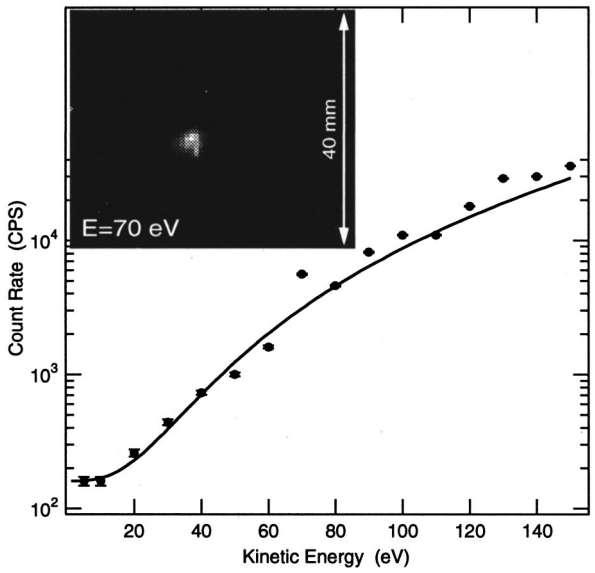

FIG. 2. Performance test of the electron gun. The count rate on a logarithmic scale is shown as function of the cathode potential (symbols). The line serves as a guide to the eye. Inset: image of the electron spot at $E=70$ eV and at a distance of 65 mm from the source.

II. DESIGN OF THE ELECTRON GUN

Common to all designs of pulsed electron guns is the electron emission process. A pulsed laser beam is focused from behind onto a thin metal film, producing electrons by two-photon photoemission (2PPE). The space charge in front of the cathode possesses, thereby, the time structure of the laser pulse, and the energy distribution depends on the 2PPE spectrum of the metal. The latter is given by $2h\nu-\Phi$,[16] where $h\nu$ denotes the photon energy and Φ the work function of the cathode material. Since 2PPE is a second-order process, the obtained total charge depends on the photon intensity squared. In order to find a compromise between the total electron yield obtained from the cathode and the width of the electron energy distribution, gold has been chosen as the cathode material, gold having the further advantage of being chemically inert in ultrahigh vacuum. The Au film has been evaporated onto a 100-μm-thick mica substrate at room temperature and subsequently annealed.[17] Simultaneous monitoring of optical transmission of the laser beam through the cathode and of the electron yield during evaporation allowed the film thickness to be optimized for maximum electron output. The final parameters thus obtained are a transmittance of 5%, corresponding to a film thickness of roughly 190 Å,[18] and total photoelectron yield of up to 1 nA using 3.1 eV photons of 1 nJ per pulse and 80 MHz repetition rate.[19] After photoemission from the negatively biased cathode, the electrons are accelerated towards the grounded anode over a distance of 75 μm, ensuring a minimum time spread while maintaining the electric-field strength below the vacuum breakthrough value. The spacing between cathode and anode is fixed by a 75-μm-thick kapton foil, in the center of which a hole of 2 mm in diameter has been pierced (see the inset in Fig. 1). In preceding measurements, the isolating power of 25-μm-thick kapton foil has been found to be better than 18 kV/mm.[20]

Since in a focusing electron-optical lens electrons traveling off the optical axis take a longer time to arrive at the focal point than electrons traveling along the axis, any electron-optical element will cause additional temporal spread.[15] Therefore, a simple microchannel plate (MCP) with nonbiased channels has been chosen as a collimator filtering out electrons moving off axis. The small angular beam divergence, given essentially by the aspect ratio of the transmitting channels [800 μm length to 10 μm diam (Ref. 21)] is paid for by the low electron transmission of the order of 10^{-5} through the MCP. Ray-tracing calculations[22] confirmed that this kind of optical element preserves the electron pulse characteristics, in particular its time structure.[20]

III. PERFORMANCE

In order to test the performance of the gun we have proceeded in two steps. First, the shape and size of the electron spot, the electron yield, and energy distribution have been measured using a position-sensitive resistive anode detector with retarding copper grid at a distance of 65 mm from the gun. Results for the electron yield and a representative spot image are shown in Fig. 2. From the size of the spot, the angular beam divergence can be estimated to be less than $\pm 0.5°$ for kinetic energies below 100 eV, slightly increasing to $\pm 0.7°$ at higher energies. Note that well-defined spots have been observed for energies down to about 3 eV without shielding against magnetic fields. This emphasizes the excellent coherence of the electron beam even at the lowest energies. Applying a retarding voltage to the copper grid allows the energy spectrum to be measured. The spectrum has a full width at half maximum of 1.3 eV, in agreement with 2PPE measurements from a gold surface [$\approx$1 eV (Ref. 20)], if one takes the poor energy resolution of a single retarding grid into account. The observed count rate can directly be translated into an electron current yielding about 2 fA at 100 eV, hence, 1 electron per 6×10^3 pulses. An important limitation of low-energy electron guns is the space charge, which

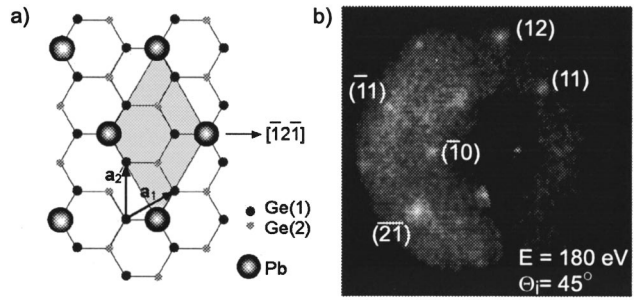

FIG. 3. LEED pattern from the Pb:Ge(111) surface obtained using the ps electron gun. (a) Hard-sphere model of the $\sqrt{3}\times\sqrt{3}R30°$ reconstruction. Ge atoms of the two topmost layers are shown as small circles, and lattice vectors a_1 and a_2 are indicated; the shaded area emphasizes the Pb-induced supercell. (b) LEED pattern taken at 180 eV in specular geometry; the diffraction orders of some spots are indicated by Miller indices referring to the 1×1 lattice vectors in (a).

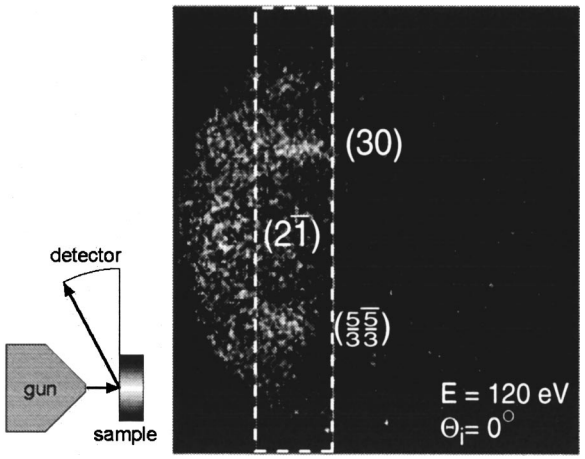

FIG. 4. LEED pattern taken in the final geometry, i.e., normal incidence and detection in grazing direction; the scattering geometry is sketched; exposure time has been 15 min. Spots are indicated as in Fig. 3; the dashed rectangle encloses the integration area of the profile shown in Fig. 5.

broadens the electron pulse.[15] In our setup, the space charge is confined in front of the cathode in a area defined by the spot size of the laser beam, about 250 μm in diameter. The maximum current from the cathode is of the order of 1 nA, corresponding to 80 electrons per pulse, two orders of magnitude less than the current leading to a 0.1 V potential gradient due to the space charge.[20] Therefore, this effect can safely be neglected.[15,20]

The second step has been to perform diffraction experiments using a commercial microchannel LEED detector. Since the current is smaller by roughly 8–9 orders of magnitude than those obtained from conventional electron sources, the diffracted beams have to be integrated over several minutes. In our setup, spherical four-grid LEED optics are used, followed by two MCP mounted in chevron configuration.[23] The MCP amplified current is visualized on a planar fluorescent screen, and the light spots are recorded by a Peltier-cooled charge-coupled-device (CCD) camera. One representative LEED image, taken in specular reflection from a Pb $\sqrt{3}\times\sqrt{3}R30°$ Ge(111) surface at room temperature,[24,25] is shown in Fig. 3 beside a hard-sphere model of the surface. The image has been integrated over 6 min, and a reference image, recorded over the same exposure time and with positive cathode bias ($\approx$10 V), has been subtracted. Except for intensity, it is comparable to images obtained using conventional electron guns with thermally activated cathode and electrostatic lens system.

Since the time spread of the electron pulse increases with increasing cathode–sample distance, the latter is limited to 4 mm in order to obtain temporal resolution of 5 ps. Furthermore, in future time-resolved experiments, the sample has to oriented for normal incidence in order to avoid path length differences (see inset in Fig. 4). The LEED optics then allows the reflected electrons to be detected within 55°–90° in scattering angle. For a minimum active cathode area of 250 μm, the incidence angle has to be controlled to better than 5° to ensure a time spread below 5 ps.[26] A LEED image, taken in this geometry, is shown in Fig. 4. The exposure time has been 15 min owing to the weaker intensity of higher-order diffraction spots.

Analysis of the signal statistics of a smooth background and of uniformly illuminated images reveals that the CCD camera detects roughly ten events per electron entering the detector. Supposing that this ratio is independent of the signal intensity, the true electron count rate can be calculated. We obtain 20–30 electrons per second for a typical LEED spot in normal-incidence geometry with a signal-to-background ratio of 2:1 (see Fig. 5). Thus, in order to detect a 1% intensity change, one needs a minimum integration time of about 7 min per image.

IV. DISCUSSION

A new design for a low-energy electron gun working without an electron-optical lens element is presented. The time resolution, which can be achieved with this type of gun, should be below 5 ps at 100 eV kinetic energy. First test measurements with a single-electron detector show that the gun provides enough electrons to record LEED images on a reasonable time scale for pump–probe experiments and demonstrate the high coherence of the electron beam, that is,

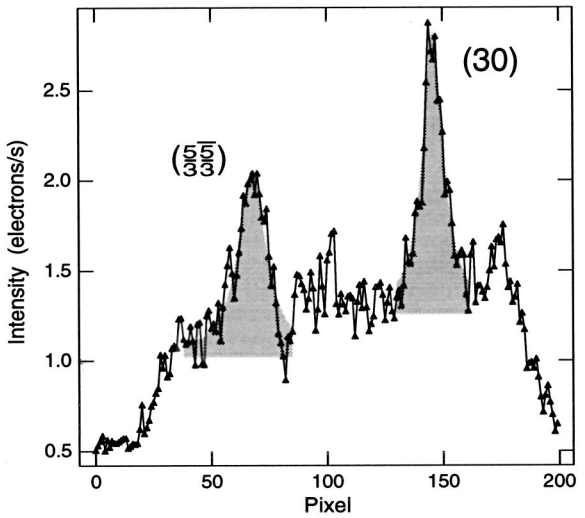

FIG. 5. Spot profile from two spots of the image shown in Fig. 4. Note that only a reference image has been subtracted. Integration of the peak intensities (shaded areas) yields 20 electron per second in either spot.

with a spread in energy and angle small enough to record the interference pattern.[12] *I–V* curves have successfully been measured in specular geometry by taking images at discrete energies and integrating the spot intensities numerically, emphasizing again the versatility of the gun. The scope of this gun, however, is not limited to electron diffraction, and we want to point out that other methods like electron energy-loss spectroscopy with picosecond time resolution could be conceivable in the near future.

ACKNOWLEDGMENTS

The authors gratefully acknowledge the skillful assistance of our mechanical workshop, in particular, B. Wachter and U. Notter (ETH Zürich) for cutting the MCPs. The authors benefited from valuable discussion with M. Hegner concerning the gold films. This work is supported by the Swiss National Science Foundation.

[1] C. V. Shank, R. Yen, and C. Hirlimann, Phys. Rev. Lett. **51**, 900 (1983).
[2] C. Rischel, A. Rousse, I. Uschmann, P.-A. Albouy, J.-P. Geindre, P. Audebert, J.-C. Gauthier, E. Förster, J.-L. Martin, and A. Antonetti, Nature (London) **390**, 490 (1997).
[3] C. Rose-Petruck, R. Jimenez, T. Guo, A. Cavalleri, C. W. Siders, F. Ráksi, J. A. Squier, B. C. Walker, K. R. Wilson, and C. P. J. Barty, Nature (London) **398**, 310 (1999).
[4] C. W. Siders, A. Cavalleri, K. Sokolowski-Tinten, Cs. Tóth, T. Guo, M. Kammler, M. Horn von Hoegen, K. R. Wilson, D. von der Linde, and C. P. J. Barty, Science **286**, 1340 (1999).
[5] A. H. Chin, R. W. Schoenlein, T. E. Glover, P. Balling, W. P. Leemans, and C. V. Shank, Phys. Rev. Lett. **83**, 336 (1999).
[6] A. M. Lindenberg, I. Kang, S. L. Johnson, T. Missalla, P. A. Heiman, Z. Chang, J. Larsson, P. H. Bucksbaum, H. C. Kapteyn, H. A. Padmore, R. W. Lee, J. S. Wark, and R. W. Falcone, Phys. Rev. Lett. **84**, 111 (2000).
[7] L. X. Chen, W. J. H. Jäger, G. Jennings, D. J. Gosztola, A. Munkholm, and J. P. Hessler, Science **292**, 262 (2001).
[8] H. E. Elsayed-Ali and G. A. Mourou, Appl. Phys. Lett. **52**, 103 (1988); H. E. Elsayed-Ali and J. W. Herman, *ibid.* **57**, 1508 (1990).
[9] M. Aeschlimann, E. Hull, C. A. Schmuttenmaer, J. Cao, Y. Gao, D. A. Mantell, and H. E. Elsayed-Ali, Proc. SPIE **2521**, 103 (1995).
[10] H. Ihee, J. Cao, and A. H. Zewail, Chem. Phys. Lett. **281**, 10 (1997); H. Ihee, V. A. Lobastov, U. M. Gomez, B. M. Goodson, R. Srinivasan, C.-Y. Ruan, and A. H. Zewail, Science **291**, 458 (2001).
[11] X. Zeng, B. Lin, I. El-Kholy, and H. E. Elsayed-Ali, Phys. Rev. B **59**, 14907 (1999).
[12] J. B. Pendry, in *Low Energy Electron Diffraction*, edited by G. K. T. Conn and K. R. Coleman, Techniques of Physics Series (Academic, London, 1974).
[13] A. M. Lahee, J. P. Toennies, and C. Wöll, Surf. Sci. **177**, 371 (1986).
[14] K. A. Merchant, D. E. Thompson, and M. D. Fayer, Phys. Rev. Lett. **86**, 3899 (2001).
[15] P. M. Weber, S. D. Carpenter, and T. Lucza, Proc. SPIE **2521**, 23 (1995); J. R. Thompson, P. M. Weber, and P. J. Estrup, *ibid.* **2521**, 113 (1995).
[16] W. Steinmann, Appl. Phys. A: Solids Surf. **49**, 365 (1989).
[17] M. Hegner, P. Wagner, and G. Semenza, Surf. Sci. **291**, 39 (1993). Some of the Au/mica films have been examined by means of scanning tunneling microscopy; they exhibited large, atomically flat terraces.
[18] This estimation is based on the following optical constants for Au thin films and 400 nm wavelength: absorption coefficient 1.06×10^{6} cm^{-1}, calculated from M.-L. Thèye, Phys. Rev. B **2**, 3060 (1970); refractive indices 1.45 for Au and 1.6 for mica, values taken from *Handbook of Optics*, edited by W. G. Driscoll and W. Vaughan (McGraw-Hill, New York, 1978).
[19] Commercial Ti:sapphire based laser, 800 nm mean wavelength, 80 MHz repetition rate, frequency doubling by BBO crystal; the pulse length at 400 nm was determined by autocorrelation to be 70 fs.
[20] R. Karrer, Diploma thesis, University of Zürich (2001).
[21] Burle Electro Optics Inc., Sturbridge, MA; zero-bias microchannel plates; distance between two channels 12 μm, surface resistivity 4 Ω/mm, channel resistance 25 MΩ—to avoid potential inhomogeneities the channel resistance has been shorted by conducting glue on the border of the MCP.
[22] SIMION software package, Idaho National Engineering Laboratory, EG&G Idaho Inc. Idaho Falls.
[23] OCI Vacuum Microengineering, London (Ontario), Canada.
[24] H. Huang, C. M. Wei, H. Li, B. P. Tonner, and S. Y. Tong, Phys. Rev. Lett. **62**, 559 (1989).
[25] J. M. Carpinelli, H. H. Weitering, and E. W. Plummer, Surf. Sci. **401**, L457 (1998); J. M. Carpinelli, H. H. Weitering, E. W. Plummer, and R. Stumpf, Nature (London) **381**, 398 (1996), and references therein.
[26] The sample is mounted on a two-axis goniometer allowing the azimuthal and polar orientation of the sample to be controlled to better than 0.1° over the full range of the hemisphere; see T. Greber, O. Raetzo, T. J. Kreutz, P. Schwaller, W. Deichmann, E. Wetli, and J. Osterwalder, Rev. Sci. Instrum. **68**, 4549 (1997).